Journal of Molecular Graphics and Modelling 72 (2017) 50–57

Contents lists available at ScienceDirect

Journal of Molecular Graphics and Modelling

journal homepage: www.elsevier.com/locate/JMGM

# Computational study for the circular redox reaction of $N_2O$ with CO catalyzed by fullerometallic cations $C_{60}Fe^+$ and $C_{70}Fe^+$

Maryam Anafcheh [a], Fereshteh Naderi [b], Zahra Khodadadi [c], Fatemeh Ektefa [c], Reza Ghafouri [c,*], Mansour Zahedi [d]

[a] Department of Chemistry, Alzahra University, Vanak, 19835-389, Tehran, Iran
[b] Department of Chemistry, Shahr-e-Qods Branch, Islamic Azad University, Tehran, Iran
[c] Department of Applied Chemistry, South Tehran Branch, Islamic Azad University, Tehran, Iran
[d] Department of Chemistry, Faculty of Sciences, Shahid Beheshti University, Evin, 19839-63113, Tehran, Iran

ARTICLE INFO

*Article history:*
Received 19 August 2016
Received in revised form 2 December 2016
Accepted 29 December 2016
Available online 31 December 2016

*Keywords:*
Fullerometallic cation
Redox reaction
Catalyst
DFT

ABSTRACT

We applied density functional calculations to study the circular redox reaction mechanism of $N_2O$ with CO catalyzed by fullerometallic cations $C_{60}Fe^+$ and $C_{70}Fe^+$. The on-top sites of six-membered rings ($\eta^6$) of fullerene cages are the most preferred binding sites for $Fe^+$ cation, and the hexagon to pentagon migration of $Fe^+$ is unlikely under ambient thermodynamic conditions. The initial ion/molecule reaction, $N_2O$ rearrangement and $N_2$ abstraction on the considered fullerometallic cations are easier than those on the bare $Fe^+$ cation in the gas phase. Generally, our results indicate that fullerometallic ions, $C_{60}Fe^+$ and $C_{70}Fe^+$, are more favorable substrates for redox reaction of $N_2O$ with CO in comparison to the other previously studied carbon nanostructures such as graphene and nanotubes.



## 1. Introduction

Conversion of hazardous gasses produced in fossil-fuel combustion, such as carbon monoxide and nitrous oxide into carbon dioxide and nitrogen molecule, are of utmost importance both environmentally and economically [1,2]. While this oxidation-reduction (redox) reaction is exothermic, $\Delta_r H = -357$ kJ/mol for the process $N_2O + CO \rightarrow N_2 + CO_2$, it does not occur directly to any measurable extent at either room or elevated temperatures, because of high energy barrier that exceeds 193 kJ/mol for the $N_2O$/CO couple [2,3]. Therefore, catalytic converters such as atomic transition metal cations, metal oxides, mixed metaloxide compounds, supported metal catalysts, metal zeolites, and alloys have all been investigated as catalysts, required to remove these undesirable pollutants [4].

Over the past few decades, numerous investigations have been focused on the role of bare atomic transition metal cations and metal-oxide ion clusters in the catalytic reduction of $N_2O$ molecule by CO [5–10]. The first example of a homogeneous catalysis in the gas phase, whereby atomic transition metal cations bring about the efficient reduction of $N_2O$ by O-atom transport, was reported in a landmark study by Kappes and Staley [5], followed by numerous experimental and theoretical investigations[11,12]. They observed that an $Fe^+$ ion transports an oxygen atom from $N_2O$ to CO in the process $N_2O + CO \rightarrow N_2 + CO_2$. Böhme and Schwarz [4] reviewed gas-phase catalytic reactions mediated by atomic metal ions, metal oxide cations, and cluster ions under thermal conditions. For example, the thermal reactions for the formation of diatomic metal oxides with $N_2O$ as an oxidant were investigated for 59 atomic cations. Only 10 of these 59 atomic cations, namely $Ca^+$, $Fe^+$, $Ge^+$, $Sr^+$, $Ba^+$, $Os^+$, $Ir^+$, $Pt^+$, $Eu^+$, and $Y^+$, were observed to have catalytic activity [4]. Recently, Lin et al. [13] theoretically investigated the effect of doublet and quartet states of Rh and singlet, triplet, and quintet of $Rh^+$ on the catalytic O-atom transport in the reduction of $N_2O$ by CO, adding $Rh^+$ ions to the list of catalysts active in the reduction of $N_2O$ by CO. Among the theoretical studies, Gao et al. [14] examined the circular reaction mechanisms of $N_2O$ with CO catalyzed by doublet and quartet states of $PtO^+$ based on the ab initio calculations. Wang et al. [15] showed that catalytic room temperature oxidation of CO by $N_2O$ can be mediated by the bimetallic oxide cluster couple $[AlVO_4]^+/[AlVO_3]^+$ [9]. In view of the doping effects in the gas-phase reactions of heteronuclear cluster oxides, Ma et al. [2] investigated the $[YAlO_2]^+/[YAlO_3]^+$ and $[Y_2O_2]^+/[Y_2O_3]^+$ couples in the context of $N_2O$/CO conversion. Their experimental/computational findings showed the low cat-

* Corresponding author.
*E-mail address:* reghafouri@gmail.com (R. Ghafouri).

http://dx.doi.org/10.1016/j.jmgm.2016.12.016
1093-3263/

alytic activities of the structurally related cluster ions $[YAlO_n]^+$ and $[Y_2O_n]^+$ (n = 2, 3) in the redox reactions with $N_2O$/CO.

The role of carbon materials in heterogeneous catalysis were discussed in literature [16,17]. For example, the reactivity of the $Fe^+$ cation was observed to be enhanced by its attaching to the carbonaceous ligands such as ethylene and cyclopentadiene [18]. Blagojevic et al. [11] investigated the effect of benzene on the catalytic O-atom transport by $Fe^+$ in the reduction of $N_2O$ by CO. On the other hand, the possibility of use of fullerene family compounds, carbon nanotubes and carbon nanofibers as carriers in heterogeneous catalysis was also noted [19], however, their properties differ sharply from those of conventional carbonaceous ligands [20–22]. Actually, catalysis can be one of the most promising applications of fullerenes and fullerene-containing materials [23].

Fullerene molecules have relatively large molecular sizes (0.7–1.0 nm) with a closed surface devoid of substituents. They are π-systems involving a closed n-electron shell with all bonds unsaturated responsible for the high polarizability of these molecules [21,24]. Endohedral complexes of carbon fullerene cages show great interest both for theorists and experimentalists [25]. As regards the possible area of practical importance, general interest is focused primarily on the superconductive property of the fullerene-alkali metal system at a rather high critical temperature, around 33 K [23–26]. On the other hand, the unsaturated character of fullerenes enables them to participate as ligands of varying hapticity in various exohedral complexes of fullerenes. Several possibilties can be envisaged: $\eta^1$, simple σ-binding at a single vertex; $\eta^2$, π-complex at an edge or geometrically equivalent twofold σ-binding at neighboring vertices; $\eta^3$, π-allyl binding; $\eta^4$, π-complex of the trimethylenemethane or 1,3-diene type; $\eta^5$, π-cyclopentadienyl complex; $\eta^6$, π-arene complex. Coordination modes and different hapticities for fullerene organometallic complexes were reviewed by Delia Soto and Roberto Salcedo [27]. Among these, $\eta^5$-π-cyclopentadienyl and $\eta^6$-π-arene complexes of fullerene suggests of a new promising field combining fullerene and coordination chemistry playing an important role in catalysis [21]. A qualitative analysis by Gal'pern et al. [28] showed that both $\eta^5$-π- and $\eta^6$-π-complexes of the fullerene with transition metals are less stable than classical sandwich-type complexes involving cyclopentadienyl and benzene. Kochkanyan et al. [29] reported synthesis of iron-containing carbon cages by reaction of $C_{60}$ fullerene with ferrocene. Bulina e al. [24] demonstrated that chromatographic separation of a fullerene mixture containing iron clusters makes it possible to isolate individual fullerenes containing a particular type of clusters. Fullerene and iron ($C_{60}$+Fe) mixture plasmas were studied in the ECR discharge ion source by Fekete et al. [30]. Matsuo et al. [31] described a molecular photoelectric switch fabricated on indiumtin oxide (ITO) as a self-assembled monolayer (SAM). On the other hand, Caraiman et al. [32] measured the reactivities of $C_{60}Fe^+$ and $C_{20}H_{10}Fe^+$ with several small inorganic and organic molecules in helium bath gas at 0.35 Torr using a selected-ion flow tube (SIFT) mass spectrometer. Comparisons with measured reactivities of the bare $Fe^+$ ion indicated that the presence of $C_{60}$ and $C_{20}H_{10}$ leads to enhancements in reactivity at room temperature up to 5 orders of magnitude [33]. The oxidation mechanism of CO to $CO_2$ catalyzed by Fe-porphyrin using $N_2O$ as an oxidizing agent was studied by Pornsatitworakul et al. [34]. Their computational results predicted that the reaction could process under ambient condition and the Fe-porphyrin could be a potential catalyst for the reduction of $N_2O$ and the oxidation of CO for the environmental implication. Moreover, it is worthy noted that reactions of $Fe^+$ attached to carbonaceous ligands are also of interest in the chemistry of dense interstellar clouds. For example, iron carbonyls are supposed to be present in the interstellar dust [35], in molecular clouds [36,37] and were detected in certain meteorite type [38]. Garcia-Hernandez et al. [39] synthesized the fullerene iron carbonyl complexes $[Fe(CO)_4(\eta^2C_{60})]$ and $[Fe(CO)_4(\eta^2C_{70})]$ in high yields by photochemical irradiation of benzene solutions of $C_{60}$ or $C_{70}$ fullerenes in presence of $Fe(CO)_5$. Also, a multistep process, involving the generation of $Fe^+$ by laser desorption from an iron target, reaction of $Fe^+$ with gaseous pentane to form $Fe(C_nH_{2n})^+$ ($n$ = 2–5) and subsequent ligand exchange with gaseous $C_{60}$ or $C_{70}$, was reported to produce $C_{60}Fe^+$ and $C_{70}Fe^+$, isolated by ion cyclotron resonance techniques [40].

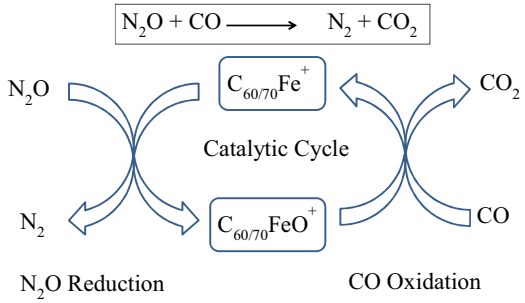


**Fig. 1.** Schematic representation of circular redox reaction mechanism of $N_2O$ with CO catalyzed by fullerometallic cations $C_{60}Fe^+$ and $C_{70}Fe^+$.

Therefore, it would be a good idea to investigate the circular redox reaction mechanism of $N_2O$ with CO catalyzed by fullerometallic ions $C_{60}Fe^+$ and $C_{70}Fe^+$ based on density functional theory (DFT) calculations. In the present work, we investigate the effect of $C_{60}$ and $C_{70}$ fullerenes on the catalytic O-atom transport by $Fe^+$ cation to address these questions: Are the reactivity of the $Fe^+$ cation could be enhanced by attaching it to the fullerene? Could $C_{60}Fe^+$ or $C_{70}Fe^+$ be favorable catalysts for the reduction of $N_2O$ and the oxidation of CO? How does the existence of the $C_{60}$ or $C_{70}$ affect the exothermicity and energy barrier of the mentioned reaction?

## 2. Computational details

The equilibrium geometries of all the stationary points (reactants, products, and transition states) were optimized at the restricted or unrestricted M06-2X [41] level with the 6–311 + G(d, p) basis set. The M06-2X functional belongs to a family of hybrid meta-generalized-gradient-approximation exchange-correlation functionals, which includes an accurate treatment of the dispersion energy [41]. Recent studies revealed that this combination of basis set with the functional provides accurate results on the fullerenes and nanotubes [41–46]. Corresponding vibrational frequencies were computed in the harmonic approximation to identify equilibrium and transition structures. All the transition state structures were characterized by exhibiting the existence of a single frequency mode associated with a pure imaginary frequency. Intrinsic reaction coordinates (IRC) calculations were used to connect transition states with reactants and products. All DFT calculations were performed using GAMESS suite of programs [47].

## 3. Results and discussions

As seen from Fig. 1, catalytic conversion of carbon monoxide and nitrous oxide into carbon dioxide and nitrogen molecule can be viewed as a circular redox reaction. In the presence of $N_2O$, the fullerometallic ions $C_{60}/C_{70}Fe^+$ bring about the reduction of $N_2O$ by O-atom transport, and $C_{60}/C_{70}Fe^+$ is oxidized to $C_{60}/C_{70}FeO^+$, and if CO is added, the reverse reaction occurs. It must be noted that the initial configuration of an $Fe^+$ cation on the fullerene surface can be effected the subsequent catalytic reactions. Hence, to better understand the catalytic reactivity of the $C_{60}/C_{70}Fe^+$ fullerometallic ions, it would be interesting to investigate the adsorption of an $Fe^+$ cation on the surface of the fullerenes $C_{60}$ and $C_{70}$. Considering the various

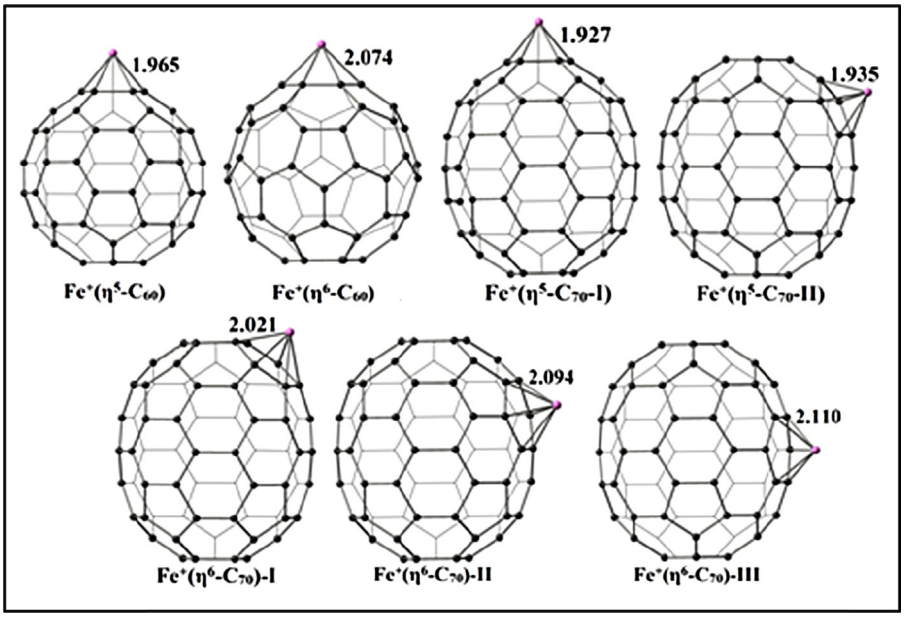


**Fig. 2.** Optimized structures of different adsorption configurations of an $Fe^+$ cation on the surface of the fullerenes $C_{60}$ and $C_{70}$, $Fe^+(\eta^6\text{-}C_{60}/C_{70})$ and $Fe^+(\eta^5\text{-}C_{60}/C_{70})$, along with their corresponding structural parameters.

**Table 1**
Total energies ($E_T$ in eV), relative ($E_r$ in eV), binding ($E_b$ in eV) energies, C-Fe bond lengths (in Ångstrom) and natural atomic charges of Fe (q(Fe) in $Q/e$ ($e = 1.6 \times 10^{-19}$C) of different isomers of the $C_{60}/C_{70}Fe^+$ fullerometallic ions.

| | ET | Er | Eb | C-Fe | q(Fe) |
|---|---|---|---|---|---|
| $Fe^+(\eta^5\text{-}C_{60})$ | −3531.04788 | 0.70 | 4.02 | 1.965 | 1.282 |
| $Fe^+(\eta^6\text{-}C_{60})$ | −3531.06371 | 0 | 4.72 | 2.074 | 1.343 |
| $Fe^+(\eta^5\text{-}C_{70})$-I | −3910.13267 | 1.52 | 4.42 | 1.927 | 1.287 |
| $Fe^+(\eta^5\text{-}C_{70})$-II | −3910.1349 | 1.47 | 4.48 | 1.935 | 1.275 |
| $Fe^+(\eta 6\text{-}C_{70})$-I | −3910.1397 | 0.51 | 5.43 | 2.021 | 1.331 |
| $Fe^+(\eta^6\text{-}C_{70})$-II | −3910.15047 | 0.22 | 5.72 | 2.094 | 1.390 |
| $Fe^+(\eta 6\text{-}C_{70})$-III | −3910.15861 | 0 | 5.94 | 2.110 | 1.426 |

possible adsorption configurations, two different binding sites are considered for the $Fe^+$ cation: the on-top site of a six-membered ring and the on-top site of a five-membered ring. The optimized structures of $Fe^+(\eta^6\text{-}C_{60}/C_{70})$ and $Fe^+(\eta^5\text{-}C_{60}/C_{70})$ along with their corresponding structural parameters are indicated in Fig. 2. Binding energies are calculated as follows:

$$E_b = E(C_{60}/C_{70}) + E(Fe^+) - E(C_{60}/C_{70}Fe^+) \quad (1)$$

where $E(C_{60}/C_{70}Fe^+)$ is the total energy of the system composed of a fullerene and an $Fe^+$ cation; $E(C_{60}/C_{70})$ and $E(Fe^+)$ are the total energies of the pristine fullerene and an isolated $Fe^+$ cation, respectively. Systems with larger binding energies are more stable. The important geometrical parameters, total energies ($E_T$), relative ($E_{rel}$) and binding ($E_b$) energies of different isomers of the $C_{60}/C_{70}Fe^+$ fullerometallic ions are listed in Table 1. The distances of C and Fe at the on-top site of a six-membered ring, $Fe^+(\eta^6\text{-}C_{60}/C_{70})$, and Fe at the on-top site of a five-membered rings, $Fe^+(\eta^5\text{-}C_{60}/C_{70})$, are found to be 2.021–2.110 and 1.927–1.965 Å, respectively, compared to typical C–Fe distances (2.041–2.145 Å) in organoiron compounds [48]. The computed binding energies for the $Fe^+(\eta^5\text{-}C_{60})$ and $Fe^+(\eta^6\text{-}C_{60})$ are obtained to be 4.02 and 4.72 eV, respectively. According to the $D_{5h}$ symmetry, a $C_{70}$ cage has three nonequivalent six-membered rings and two distinct kinds of five-membered rings, see Fig. 2. Note that the most stable isomer is $Fe^+(\eta^6\text{-}C_{70})$-III, where $Fe^+$ is added to the on-top site of a six-membered ring at the equatorial region of $C_{70}$, followed by $Fe^+(\eta^6\text{-}C_{70})$-II and $Fe^+(\eta^6\text{-}C_{70})$-I while $Fe^+(\eta^5\text{-}C_{70})$-II and $Fe^+(\eta^5\text{-}C_{70})$-I have the fourth and fifth lowest binding energies. Our results are in line with those previously reported for graphene and carbon nanotubes [49,50]. In general, our calculations showed that the on-top site of a six-membered ring ($\eta^6$) of fullerene cages is the most preferred binding site for $Fe^+$ ion, and also is more favorable than the six-membered ring ($\eta^6$) of graphene or carbon nanotubes, which can be attributed to the high electroafinity, high curvature, and different cation–$\pi$ interaction in the fullerenes. These results are also in agreement with those reported by Kandalam et al. [33] on the Corannulene, $C_{20}H_{10}$. The energy barrier when the $Fe^+$ cation moves from the on-top site of a six-membered ring of $C_{60}$ to the on-top site of a five-membered ring across a C—C bridge is calculated to be 2.81 eV. This barrier is larger than those reported previously in the carbon nanotubes when a metal atom or cation moves across a C—C bridge [18,49]. Because this is much larger than the thermal energy corresponding to the room temperature (1.4 eV), $Fe^+$ migration is unlikely under ambient thermodynamic conditions.

Since the $C_{60}$ core (and $C_{70}$) is very efficient electron acceptor, so it will be attract the electron density from $Fe^+$ cation. In order to obtain a quantitative understanding of the electric charges influence on the chemical reaction initiation, we also perform natural population analysis, (NPA) [51] on the wave functions calculated at the same level of the theory [52]. The natural charge analysis of the $C_{60}Fe^+$ and $C_{70}Fe^+$ fullerometallic ions shows a net charge in $Q/e$ ($e = 1.6 \times 10^{-19}$C) of +1.275–1.426 on the $Fe^+$ cation (about 0.275–0.426 e-transfer from the $Fe^+$ cation to the cages). This result indicates that the electron density on the Fe atom can transfer to the fullerene cage which acts as an electron withdrawing support. In addition, this can suggest that the Fe atom is activated to be more electrophilic by its support. The frontier molecular orbitals, HOMO and LUMO, dominantly locate on the Fe atom, see Fig. 3. The LUMO illustrates the strong d-orbitals characteristics of the Fe atom allowing an incoming electron to occupy this state. All of these observations demonstrate that the Fe atom might be the active site for adsorbing an electrophile molecule. Therefore, we expect that this positive charge around Fe atom provides suitable and strong electronic field for the initial ion/molecule reaction of $C_{60}Fe^+/C_{70}Fe^+$ with $N_2O$.

The schematic potential energy diagram of the circular redox reaction mechanism of $N_2O$ with CO catalyzed by fullerometallic

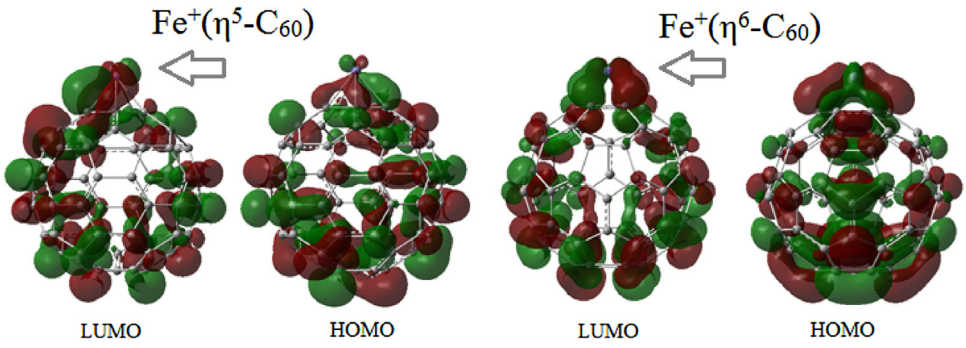


**Fig. 3.** The frontier molecular orbitals, HOMO and LUMO,of the $Fe^{+}(\eta^{5}\text{-}C_{60})$ and $Fe^{+}(\eta^{6}\text{-}C_{60})$.

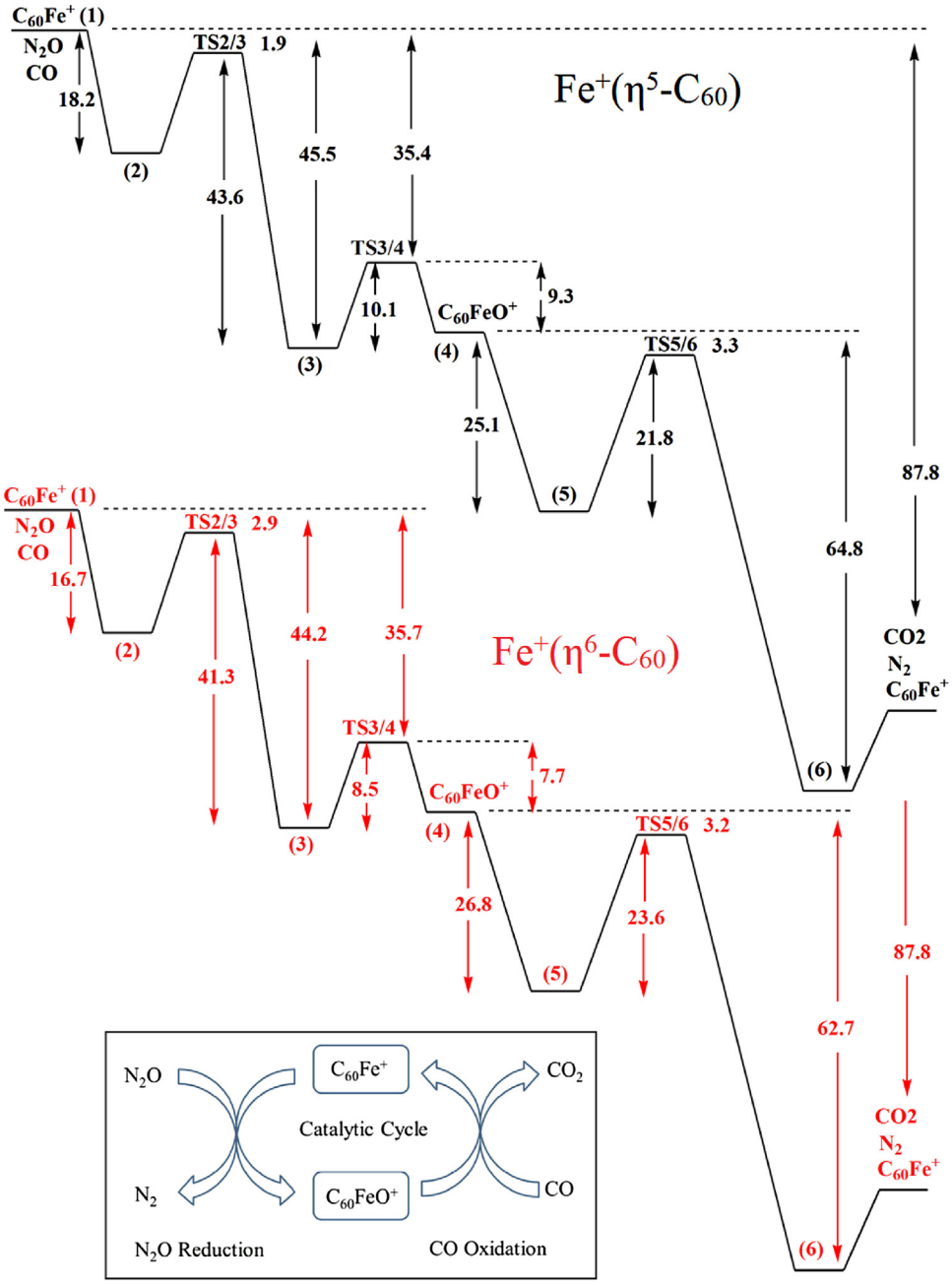


**Fig. 4.** Schematic potential energy surface (in kcal/mol) for the circular redox reaction of $N_2O$ with CO catalyzed by fullerometallic cations $Fe^{+}(\eta^{5}\text{-}C_{60})$ and $Fe^{+}(\eta^{6}\text{-}C_{60})$.

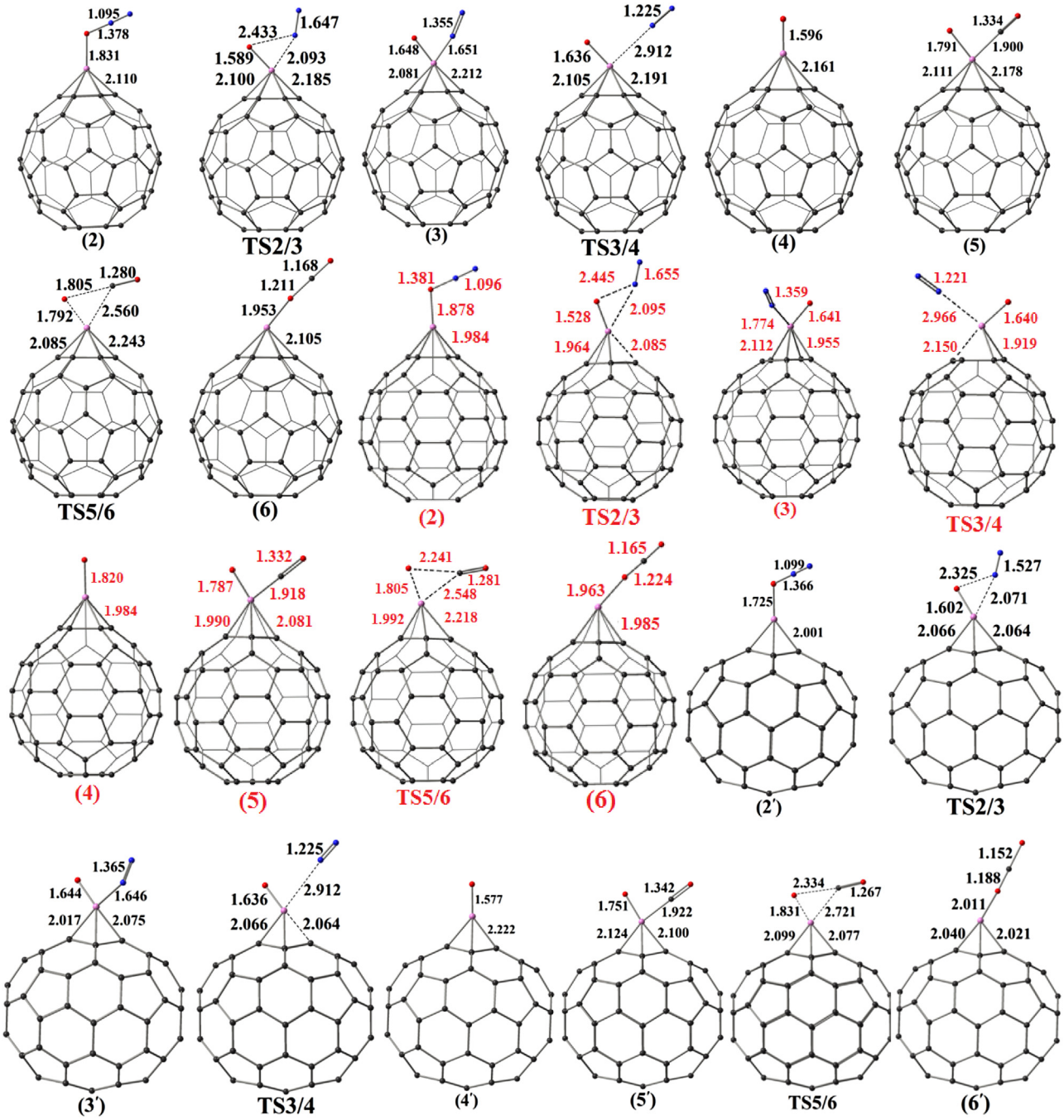


**Fig. 5.** Optimized geometries of the reactants, intermediates, transition states and products for the circular redox reaction of $N_2O$ with CO catalyzed by fullerometallic cations $Fe^+(\eta^5\text{-}C_{60})$, $Fe^+(\eta^6\text{-}C_{60})$ and $Fe^+(\eta^6\text{-}C_{70})$-III at the M06-2X/6–311 + G(d, p) level of theory. Bond lengths are in Ångstroms.

ions $C_{60}Fe^+$ with ZPE corrections obtained at the M06-2X/6-311 + G(d, p) level are plotted in Fig. 4. The optimized geometries of the reactants, products, and transition states are presented in Fig. 5. As seen, on the fullerometallic ion $C_{60}Fe^+$ (**1**) the reduction of $N_2O$ to $N_2$ starts with the adsorption of $N_2O$. In the ion/molecule reaction of **1** with $N_2O$, the isomers **2** and **3** are energetically accessible; the former corresponds to an end-on coordination of $N_2O$ to the $Fe^+$ of the $C_{60}Fe^+$ (**2**), while in the latter (**3**) the $N_2$ interacts with the $Fe^+$. The adsorption energy for the end-on coordination of $N_2O$ to the $Fe^+$ cation of the $C_{60}Fe^+$ is calculated to be about −18.2 kcal/mol which is more negative than that reported for the reaction of $N_2O$ with $Fe^+$ in the gas phase (−14.9 kcal/mol) [11] and also with that theoretically reported for Fe-Embedded Graphene (−10.0 kcal/mol) [50]. It can be explained by the contribution of π-electronic system to polarizability of the fullerometallic ions $C_{60}Fe^+$: because all C—C bonds remain unchanged in $C_{60}Fe^+$ isomers (i.e. the initial π-electronic system does not change significantly), these compounds have high polarizability which leads to the higher electrophilic properties in the $C_{60}Fe^+$ fullerometallic ions [53].

The Fe—C and Fe—O bonds in this configuration are found to be 2.110 and 1.831 Å. The N—O and N—N bond lengths of N—N—O in the complex **2** is obtained to be about 1.378 and 1.095 Å, respectively, longer than those of an isolated $N_2O$ molecule (1.186 and 0.952 Å, respectively), suggesting that adsorption process weakens the NO bond. The natural charge analysis (see Table 1) shows that an electron on the Fe atom is gained with the decrease of its positive charge

from +0.343 to +0.231, while electron density on the O atom is lost with the decrease of its negative charge from −0.111e to −0.035. The difference of the partial charges after the adsorption reveals that an electron transfers from the $N_2O$ to not only the Fe atom of −0.111, but also the $C_{60}$ cage of −0.060. In other words, the $C_{60}$ cage can significantly assist in withdrawing an electron from the $N_2O$ molecule. Then, reaction pathway can then proceed with the dissociating of N—N—O. The isomers **2** and **3** are connected by the transition structure TS2/3, which is located energetically just below the entrance channel of the separated reactants (1.9 kcal/mol, see Fig. 4). This computed activation energy (16.3 kcal/mol) shows good agreement with those reported for the reaction of $N_2O$ with bare atomic $Fe^+$ cations in the gas phase [11]. In the transition state TS2/3, the N···O bond is stretched to 2.433 Å compared with the initial N—O bond length in **2**, implying that the N···O bond is too close to be dissociated. The O atom closer to the Fe atom can accumulate more electron density by the significant increase of its negative charge from −0.035 to −0.133, whereas electron density on the Fe atom is dramatically withdrawn by the increase of its positive charge from +0.231 to +0.288. This charge transfer from the Fe atom back to the O atom might occur from the oxygen transfer from $N_2O$ to the Fe active site. In a molecular point of view, one can say that an electron was transferred from $C_{60}Fe^+$ back to the $N_2O$ to break the N—O bond. Direct loss of $N_2$ from **3** requires activation energy of 10.1 kcal/mol. Passing over TS3/4, the Fe—O bond length is continually shortened from 1.648 to 1.596 Å until the state **4** is reached. In **4**, the length of C-Fe is about 2.161 Å, longer than that in the $C_{60}Fe^+$ by 0.106 Å.

As compared to the TS3/4, electron transferring from the $C_{60}Fe$ increases the negative charge on the O atom from −0.133 to −0.248, while the positive charge on the Fe atom increases from +0.288 to +0.309, and the charge on the $C_{60}$ cage is reversed from the negative charge of −0.060 to the positive charge of +0.066. This observation indicates that the oxygen atom can strongly pull the charge back from the $C_{60}Fe$ due to its strong electronegativity. Therefore, the CO molecule can be oxidized by the $C_{60}FeO^+$ due to not only the strong negative charge on the O atom of the intermediate which can attract the C atom of the CO, but also the Fe atom which can receive an electron and can stabilize the intermediate, **5**. The oxidation mechanism of CO to $CO_2$ starts with the adsorption of CO on the ion complex $C_{60}FeO^+$ (**4**), and the resulting stationary structure (**5**) is shown in Fig. 5. In **5**, the length of C—O is about 1.334 Å, much longer than that in a free C=O molecule by 1.130 Å. The calculations indicate that the process of **5** → **6** is exothermic by about 39.7 kcal/mol, and an energy-barrier height of approximately 21.8 kcal/mol, relative to **5**, must be overcome. In the transition state TS5/6, the Fe···O and Fe—CO distances are stretched to 1.792 and 2.560 Å compared with the corresponding bond lengths in **5** while the length of C···O is shortened from 1.334 to 1.280 Å. Density functional theory calculations showed that only a total charge of 0.044e is delocalized on the $CO_2$ framework. Therefore, the structure **6** can be converted into the $CO_2$ and $C_{60}Fe^+$ by 21.7 kcal/mol. It is worthy noted that the gas-phase reactions between an array of carbon cluster ions and $Fe(CO)_5$ demonstrated that $C_{60}^+$ and $C_{70}^+$ display unique reactivities which has led to the formation of the $C_{60}Fe(CO)^{4+}$and $C_{70}Fe(CO)^{4+}$ [19]. Garcia-Hernandez et al. [39] synthesized fullerene iron carbonyl complexes $[Fe(CO)_4(\eta^2C_{60})]$ and $[Fe(CO)_4(\eta^2C_{70})]$ by photochemical irradiation of benzene solutions of $C_{60}$ or $C_{70}$ fullerenes in presence of $Fe(CO)_5$. However, Collision-induced dissociation (CID) of these compounds requires relatively small activation energies and results in the formation of CO, $Fe(CO)_5$, Fe and $C_{60}$ or $C_{70}$.

Since catalytic processes are commonly non-equilibrium and fullerene-iron particles are produced in situ, all their isomers may coexist in the reversible complexation/decomplexation of the catalyst with a substrate. Therefore, the schematic potential energy diagram of the reaction of $N_2O$ with CO catalyzed by fullerometallic ion $Fe^+(\eta^5\text{-}C_{60})$ with ZPE corrections obtained at the M06-2X/6–311 + G(d, p) level is plotted in Fig. 4. The optimized

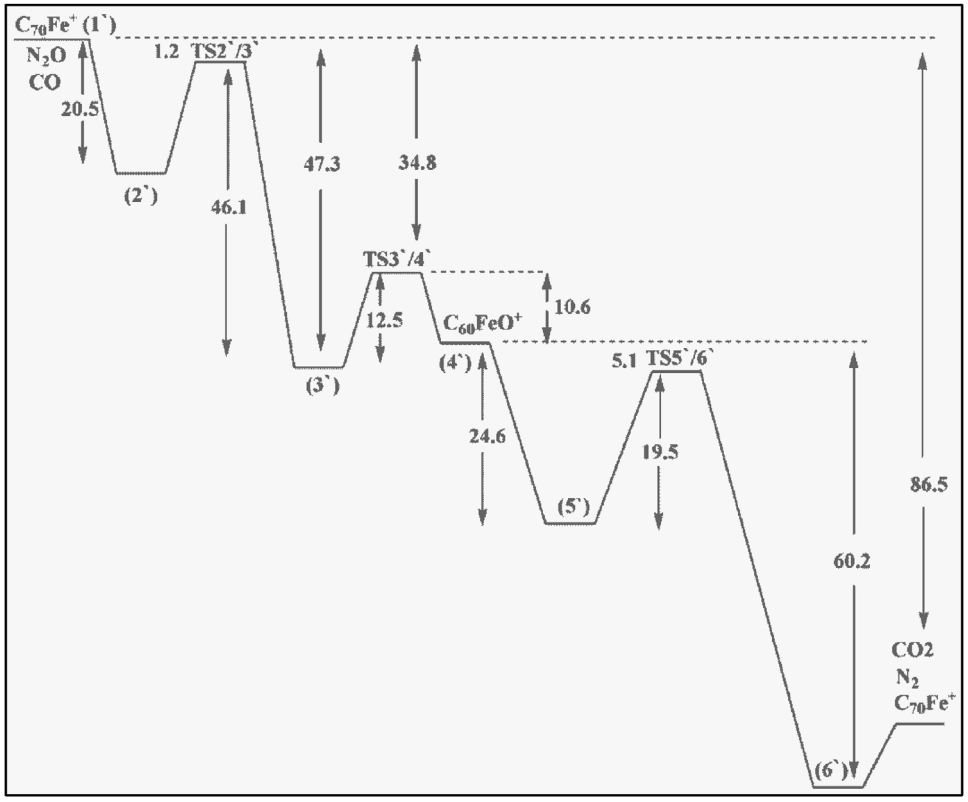


**Fig. 6.** Schematic potential energy surface (in kcal/mol) for the circular redox reaction of $N_2O$ with CO catalyzed by fullerometallic cations $Fe^+(\eta^6\text{-}C_{70})$-III.

geometries of the reactants, products, and transition states are presented in Fig. 5. The calculated adsorption energy for the end-on coordination of $N_2O$ to the Fe atom of the $Fe^+(\eta^5\text{-}C_{60})$ is about −16.7 kcal/mol which has smaller value than that calculated for the adsorption of $N_2O$ to $Fe^+(\eta^6\text{-}C_{60})$ (-18.2 kcal/mol). The geometrical parameters of newly formed bonds in the complex (**2**) are close to those obtained for $Fe^+(\eta^6\text{-}C_{60})$. The lower potential barrier heights of the processes of **2** → **3** and **3** → **4** indicate $N_2O$ rearrangement and $N_2$ abstraction on the $Fe^+(\eta^5\text{-}C_{60})$ is slightly easier than $Fe^+(\eta^5\text{-}C_{60})$. The process of **5** → **6** is exothermic by about 39.1 kcal/mol with an energy-barrier height of approximately 35.9 kcal/mol. The structure **6** can be converted into the $CO_2$ and $Fe^+(\eta^6\text{-}C_{70})$-III by 18.3 kcal/mol. However, the initial ion/molecule reaction of $Fe^+(\eta^5\text{-}C_{60})$ with $N_2O$ is less exothermic than $Fe^+(\eta^6\text{-}C_{60})$ and $N_2O$ rearrangement and $N_2$ abstraction on the $Fe^+(\eta^5\text{-}C_{60})$ is easier than $Fe^+(\eta^6\text{-}C_{60})$; the required energy for dissociation of $CO_2$ molecule is higher than $Fe^+(\eta^6\text{-}C_{60})$. In general, our results indicate that both of the fullerometallic ions $C_{60}Fe^+$ are favorable substrate for redox reaction of $N_2O$ with CO.

The schematic potential energy diagram of the reaction of $N_2O$ with CO catalyzed by fullerometallic ion $C_{70}Fe^+$ with ZPE corrections obtained at the M06-2X/6–311 + G(d, p) level is plotted in Fig. 6. The optimized geometries of the reactants, products, and transition states are presented in Fig. 5. The calculated adsorption energy for the end-on coordination of $N_2O$ to the Fe atom of the $Fe^+(\eta^6\text{-}C_{70})$-III is about −20.5 kcal/mol which is more negative than that obtained for the adsorption of $N_2O$ to $Fe^+(\eta^6\text{-}C_{60})$ (−18.2 kcal/mol). The geometrical parameters of newly formed bonds in the complex (**2'**) are close to those obtained for $Fe^+(\eta^6\text{-}C_{60})$, see Fig. 5. The higher potential barrier heights of the processes of **2'** → **3'** and **3'** → **4'** indicate $N_2O$ rearrangement and $N_2$ abstraction on the $Fe^+(\eta^6\text{-}C_{60})$ are easier than those on $Fe^+(\eta^6\text{-}C_{70})$-III. The C—Fe and Fe—O distances in the $FeO^+(\eta^6\text{-}C_{70})$-III (**4'**) are 2.222 and 1.577 Å, respectively. The process of **5'** → **6'** is exothermic by about 35.6 kcal/mol with an energy-barrier height of approximately 19.5 kcal/mol. In the transition state TS5/6, the Fe···O and Fe···CO distances are stretched to 1.831 and 2.721 Å compared with the corresponding bond lengths in **5** while the length of C···O is shortened from 1.342 to 1.267 Å. The structure **6** can be converted into the $CO_2$ and $Fe^+(\eta^6\text{-}C_{70})$-III by 19.1 kcal/mol. Since the initial ion/molecule reaction of $Fe^+(\eta^6\text{-}C_{70})$-III with $N_2O$ is more exothermic than $Fe^+(\eta^6\text{-}C_{60})$ and also the required energy for dissociation of $CO_2$ molecule is lower than the release energy in the initial ion/molecule reaction of $Fe^+(\eta^6\text{-}C_{70})$-III with $N_2O$, it is expected that redox reaction of $N_2O$ with CO Catalyzed by fullerometallic ion $C_{70}Fe^+$ is more suitable than $C_{60}Fe^+$. However, $N_2O$ rearrangement and $N_2$ abstraction on the $Fe^+(\eta^6\text{-}C_{60})$ is easier than $Fe^+(\eta^6\text{-}C_{70})$-III. In general, our results indicate that fullerometallic ions, $C_{60}Fe^+$ and $C_{70}Fe^+$, are more favorable substrates for redox reaction of $N_2O$ with CO in comparison to the other previously studied carbon nanostructures such as graphene and nanotubes.

## 4. Conclusions

In this paper, we performed a density functional study to investigate the circular redox reaction mechanism of $N_2O$ with CO catalyzed by fullerometallic ions $C_{60}Fe^+$ and $C_{70}Fe^+$. According to the obtained results, we emphasize the following points. First, the on-top site of a six-membered ring ($\eta^6$) of fullerene cages is the most preferred binding site for $Fe^+$ ion. Second, the hexagon to pentagon migration of Fe is unlikely under ambient thermodynamic conditions because of the high energy barrier. Third, the larger positive charge around Fe atom provides suitable and strong electronic field for the initial ion/molecule reaction of the considered fullerometallic ions with $N_2O$. Forth, adsorption energies for the end-on coordination of $N_2O$ to the Fe atom of the fullerometallic ions are more negative than that reported for the reaction of $N_2O$ and a bare $Fe^+$ cation. Fifth, the initial ion/molecule reaction of $Fe^+(\eta^6\text{-}C_{70})$-III with $N_2O$ is more exothermic than $Fe^+(\eta^6\text{-}C_{60})$. Sixth, the required energy for dissociation of $CO_2$ molecule is lower than the released energy in the initial ion/molecule reaction of $Fe^+(\eta^6\text{-}C_{70})$-III with $N_2O$. Therefore, it is expected that redox reaction of $N_2O$ with CO Catalyzed by the fullerometallic ion $C_{70}Fe^+$ is more suitable than $C_{60}Fe^+$. Seventh, $N_2O$ rearrangement and $N_2$ abstraction on the $Fe^+(\eta^6\text{-}C_{60})$ are easier than those on the $Fe^+(\eta^6\text{-}C_{70})$-III. Finally, our results indicate that the fullerometallic ions $C_{60}Fe^+$ and $C_{70}Fe^+$ are more favorable substrates for redox reaction of $N_2O$ with CO in comparison to the other previously studied carbon nanostructures such as graphene and nanotubes.

## Acknowledgements

We are grateful to Professor Seik Weng Ng for making us available his software (G98W) and hardware (machine time) facilities. The financial support of Research Council of Shahid Beheshti University is gratefully acknowledged.

## References

[1] U.S. Greenhouse Gas Inventory Report, Environmental Protection Agency, 2009 http://tinyurl.com/emissionsreport.
[2] J.-B. Ma, Z.-C. Wang, M. Schlangen, S.-G. He, H. Schwarz, On the origin of the surprisingly sluggish redox reaction of the $N_2O$/CO couple mediated by $[Y_2O_2]^+$ and $[YAlO_2]^+$ cluster ions in the gas phase, Angew. Chem. Int. Ed. 52 (2013) 1226–1230.
[3] H.-J. Freund, G. Meijer, M. Scheffler, R. Schlçgl, M. Wolf, CO oxidation as a prototypical reaction for heterogeneous processes, Angew. Chem. 123 (2011) 10242–10275.
[4] D.K. Böhme, H. Schwarz, Gas-phase catalysis by atomic and cluster metal ions: the ultimate single-site catalysts, Angew. Chem. Int. Ed. 44 (2005) 2336–2354.
[5] M.M. Kappes, R.H. Staley, Gas-phase oxidation catalysis by transition-metal cations, J. Am. Chem. Soc. 103 (1981) 1286–1287.
[6] S.M. Vesecky, P.J. Chen, X. Xu, D.W. Goodman, Evidence for structure sensitivity in the high pressure CO + NO reaction over Pd(111) and Pd(100), J. Vac. Sci. Technol. A 13 (1995) 1539–1543.
[7] K.C. Taylor, Nitric oxide catalysis in automotive exhaust systems, Catal. Rev. Sci. Eng. 35 (1993) 457–481.
[8] S.M. Vesecky, D.R. Rainer, D.W. Goodman, Basis for the structure sensitivity of the CO + NO reaction on palladium, J. Vac. Sci. Technol. A 14 (1996) 1457–1463.
[9] B.J. Brosilow, R.M. Ziff, Comment on NO-CO reaction on square and hexagonal surfaces: a Monte Carlo simulation, J. Catal. 136 (1992) 275–278.
[10] K. Shanmugapriya, H.-S. You, H.-C. Lee, D.R. Park, J.-S. Lee, C.W. Lee, A study of NO + CO reaction over various supported catalysts in the presence of $O_2$ and $H_2O$, Bull. Korean Chem. Soc. 28 (2007) 1039–1041.
[11] V. Blagojevic, G. Orlova, D.K. Bohme, Gas-phase O-Atom transport catalysis by atomic cations: reduction of $N_2O$ by CO, J. Am. Chem. Soc. 127 (2005) 3545–3555.
[12] M. Schlangen, H. Schwarz, Effects of ligands cluster size, and charge state in gas-phase catalysis: a happy marriage of experimental and computational studies, Cat. Lett. 142 (2012) 1265–1278.
[13] T.-S. Lin, H.-T. Chen, Computational study for the circular reaction mechanisms of $N_2O$ with CO catalyzed by rh and $Rh^+$, J. Phys. Chem. C 119 (2015) 449–455.
[14] L.-G.G. Ao, X.L. Song, Y.-C. Wang, L.-L. Lv, Theoretical investigation on the reaction of $N_2O$ and CO catalyzed by $PtO^+$, Comp. Theor. Chem. 968 (2011) 31–38.
[15] Z.-C. Wang, N. Dietl, R. Kretschmer, T. Weiske, M. Schlangen, H. Schwarz, Catalytic redox reactions in the CO/$N_2O$ system mediated by the bimetallic oxide-cluster couple $AlVO_3^+$/$AlVO_4$, Angew. Chem. Int. Ed. 50 (2011) 12351–12354.
[16] N.F. Goldshleger, Fullerenes and fullerene-based materials In catalysis, Fullerene Sci. Technol. 9 (2001) 255–280.
[17] E. Auer, A. Freund, J. Pietsch, T.B. Tacke, General Carbons as supports for industrial precious metal catalysts, Appl. Catal. A 173 (1998) 259–271.
[18] S.F. Parker, Reactions of iron atoms with benzene, J. Phys. Chem. A 114 (2010) 1657–1664.
[19] A.L. Balch, M. Olmstead, Reactions of transition metal complexes with fullerenes ($C_{60}$ $C_{70}$, etc.) and related materials, Chem. Rev. 98 (1998) 2123–2165.
[20] B. Coq, J.M. Planeix, V. Brotons, Fullerene-based materials as new support media in heterogeneous catalysis by metals, Appl. Catal. A: Gen. 173 (1998) 175.

[21] V.I. Sokolov, The problem of fullerenes, the chemical Aspects, Russ. Chem. Bull. 42 (1993) 1–11.
[22] J. Hutter, H.P. Luthi, The structure of n-Fold negatively charged $C_{60}$ (n = 1,2, . . ., 6), Int. J. Quant. Chem. 46 (1993) 81–86.
[23] H. Terrones, M. Terrones, W.K. Hsu, Beyond $C_{60}$: graphite structures for the future, Chem. Soc. Rev. 24 (1995) 341–345.
[24] N.V. Bulina, É.A. Petrakovskaya, A.V. Marachevsky, I.S. Lityaeva, I.V. Osipova, G.A. Glushchenko, W. Krätschmer, G.N. Churilov, Synthesis and investigation of iron fullerene clusters, Phys. Solid State 48 (2006) 1012–1015.
[25] A.L. Chistyakov, I.V. Stankevich, Computer simulation of molecular and electron structure of C60 fullerene complexes with twelve Half-Sandwich groups $MC_5H_5$ (M = Fe, Ru, Os), fullerenes, nanotubes and carbon nanostructures, fullerenes, nanotubes and carbon, Nanostructures 12 (2004) 425–429.
[26] W.H. Green Jr., S.M. Gorun, G. Fitzgerald, P.W. Fowler, A. Ceulemans, B.C. Titeca, Electronic structures and geometries of $C_{60}$ anions via density functional calculations, J. Phys. Chem. 100 (1996) 14892–14898.
[27] D. Soto, R. Salcedo, Coordination modes and different hapticities for fullerene organometallic complexes, Molecules 17 (2012) 7151–7168.
[28] E.G. Gal'pern, N.P. Gambaryan, L.V. Stankevich, A.L. Chistyakov, Fullerene $C_{60}$ as a rl s- and q6-1igand in sandwich-type −eomplexes with transition metals, Russ. Chem. Bull. 43 (1994) 547–550.
[29] R.O. Kochkanyan, M.M. Nechitailov, P. Byszewski, A.N. Zaritovskii, A.F. Popov, Synthesis of new iron-containing carbon cages by reaction of $C_{60}$ fullerene with ferrocene russ, J. Org. Chem. 40 (2004) 957–961.
[30] E. Fekete, S. Biri, I. Iván, Investigation of iron-fullerene mixture plasmas in ECR discharge, fullerenes, nanotubesand carbon, Nanostructures 15 (2007) 249–256.
[31] Y. Matsuo, T. Ichiki, E. Nakamura, Molecular photoelectric switch using a mixed SAM of organic [60] fullerene and [70] fullerene doped with a single iron atom, J. Am. Chem. Soc. 133 (2011) 9932–9937.
[32] D. Caraiman, G.K. Koyanagi, L.T. Scott, D.V. Preda, D.K. Bohme, Fullerometallic ion chemistry: reactions of $C_{60}Fe^+$ and $C_{20}H_{10}Fe^+$ in the gas phase, J. Am. Chem. Soc. 123 (2001) 8573–8582.
[33] A.K. Kandalam, B.K. Rao, P. Jena, DFT study of structure and binding energies of Fe-corannulene complex, J. Phys. Chem. A 109 (2005) 9220–9225.
[34] S. Pornsatitworakul, S. Phikulthai, S. Namuangruk, B. Boekfa, Proceedings 2015 International Conference on Science and Technology, TICST, 2015.
[35] A.G.G.M. Tielens, D.H. Wooden, L.J. Allamandola, J. Bregman, F.C. Witteborn, The infrared spectrum of the galactic center and the composition of interstellar dust, Astrophys. J. 461 (1996) 210–222.
[36] D.T. Halfen, L.M. Ziurys, Laboratory detection of FeCO+ (X4(−) by millimeter/submillimeter velocity modulation spectroscopy, Astrophys. J. 657 (2007) L61–L64.
[37] E. Kagi, Y. Kasai, H. Ungerechts, K. Kawaguchi, Astronomical search and laboratory spectroscopy of the FeCO radical, Astrophys. J. 488 (1997) 776–780.
[38] Y. Xu, X. Xiao, S. Sun, Z. Ouyang, IR spectroscopic evidence of metal carbonyl clusters in the Jiange H5 chondrite, Lunar Planet. Soc. Conf. 27 (1996) 1457–1458.
[39] D.A. Garcia-Hernandez, F. Cataldo, A. Manchado, About the iron carbonyl complex with $C_{60}$ and $C_{70}$ fullerene:[$Fe(CO)4(\eta^2C_{60})$] and [$Fe(CO)_4$ <($^2C_{70}$)], Fullerenes, nanotubes and carbon, Nanostruct 24 (2016) 225–233.
[40] A.L. Balch, M.M. Olmstead, Reactions of transition metal complexes with fullerenes ($C_{60}$, $C_{70}$, etc.) and related materials, Chem. Rev. 98 (1998) 2123–2165.
[41] Y. Zhao, D.G. Truhlar, The M06 suite of density functionals for main group thermochemistry thermochemical kinetics, noncovalent interactions, excited states, and transition elements: two new functionals and systematic testing of four M06-class functionals and 12 other functionals, Theor. Chem. Account. 120 (2008) 215–241.
[42] P.C. Hariharan, Accuracy of AH, equilibrium geometries by single determinant molecular orbital theory. J.A. Pople, Mol. Phys. 27 (1974) 209–214.
[43] Y. Zhang, A. Wu, X. Xu, Y. Yan, Geometric dependence of the B3LYP-predicted magnetic shieldings and chemical shifts, J. Phys. Chem. A 111 (2007) 9431–9437.
[44] R. Ghafouri, F. Ektefa, Functionalization of carbon ad-dimer defective single-walled carbon nanotubes through 1,3-dipolar cycloaddition: a DFT study, Struct. Chem. 26 (2015) 507–515.
[45] M. Anafcheh, R. Ghafouri, Mono- and multiply-functionalized fullerene derivatives through 1,3-dipolar cycloadditions: a DFT study, Phys. E 56 (2014) 351–356.
[46] M. Anafcheh, R. Ghafouri, 1,3-Dipolar cycloaddition of BC2N nanotubes: a DFT study, Comput. Theor. Chem. 1034 (2014) 32–37.
[47] M.W. Schmidt, K.K. Baldridge, J.A. Boatz, S.T. Elbert, M.S. Gordon, J.H. Jensen, S. Koseki, N. Matsunaga, K.A. Nguyen, S.J. Su, T.L. Windus, M. Dupuis, J.A. Montgomery, General Atomic, General atomic and molecular electronic structure system, J. Comput. Chem. 14 (1993) 1347–1363.
[48] Fe Organoiron Compounds: Mononuclear Compounds 9 (Gmelin Handbook of Inorganic and Organometallic Chemistry − 8th edition) 8th ed. 1985. Softcover reprint of the original 8th ed. 1985 Edition by Adolf Slawisch (Author, Editor), Jürgen Faust (Editor).
[49] H. Johll, H.C. Kang, E.S. Tok, Density functional theory study of Fe Co, and Ni adatoms and dimers adsorbed on grapheme, Phys. Rev. B 79 (2009) 245416.
[50] S. Wannakao, T. Nongnual, P. Khongpracha, T. Maihom, J. Limtrakul, Mechanisms for CO catalytic oxidation by N2O on Fe-embedded graphene, J. Phys. Chem. C 116 (2012) 16992–16998.
[51] A.E. Reed, L.A. Curtiss, F. Weinhold, Intermolecular interactions from a natural bond orbital donor-acceptor viewpoint, Chem. Rev. 88 (1988) 899–926.
[52] A.E. Reed, R.B. Weinstock, F. Weinhold, Natural population analysis, J. Chem. Phys. 83 (1985) 735–746.
[53] D. Sh Sabirov, Polarizability as a landmark property for fullerene chemistry and materials science, RSC Adv. 4 (2014) 44996–45028.